ELSEVIER

Journal of Alloys and Compounds 218 (1995) 36–43

Journal of ALLOYS AND COMPOUNDS

Mechanically assisted solid state hydrogenation for formation of nanocrystalline $NiTiH_3$ alloy powders

M. Sherif El-Eskandarany [a], H.A. Ahmed [b], K. Sumiyama [c], K. Suzuki [c]

[a] *Mining and Petroleum Engineering Department, Faculty of Engineering, Al-Azhar University, Nasr City, Cairo, Egypt*

[b] *Mining, Petroleum and Metallurgical Engineering Department, Faculty of Engineering, Cairo University, Giza, Egypt*

[c] *Institute for Materials Research, Tohoku University, Katahira 2-1-1, Sendai 980, Japan*

Received 12 July 1994

Abstract

The mechanical alloying process has been applied to preparing f.c.c. $NiTiH_3$ solid solution alloy powders using a room-temperature rod mill under a reactive hydrogen gas atmosphere. The mechanically alloyed powders have been characterized by means of X-ray diffraction, optical microscopy, scanning electron microscopy, transmission electron microscopy and chemical analysis. During the first few kiloseconds (11 ks) of the rod milling time, the coarse powder particles of Ni and Ti disintegrated into several particles that have fresh surfaces. These fresh or new surfaces are very active and able to absorb hydrogen gas, so that h.c.p. Ti reacts completely with the hydrogen gas to form f.c.c. TiH_2 with grain sizes of about 60 nm diameter. During the hydration process, the Ni powder particles are neutral and did not react with hydrogen (milling atmosphere). After a rod milling time of 43 ks, the f.c.c. TiH_2 formed diffused into Ni matrix to form f.c.c. $NiTiH_3$ solid solution with an average grain size of 10 nm diameter. This solid solution expands with increasing rod milling time (173 ks) and saturated to give a constant lattice parameter a_0 of 0.354 03 nm after milling for 360 ks. The end product of the f.c.c. $NiTiH_3$ solid solution consists of fine (1 μm in diameter) and homogeneous (spherical-like morphology) powder particles. In addition, the metallic hydride phase formed is very stable at temperatures as high as 993 K.

Keywords: Mechanical alloying; Rod milling; Solid-gas reaction; Solid state reaction; Hydration; Powder metallurgy; Metal hydrides

1. Introduction

Fundamentally, the term mechanical alloying (MA) may refer to producing homogeneous composite particles with an intimately dispersed uniform internal structure. Since 1970 [1] the MA process via the ball-milling (BM) technique has been used to prepare several dispersion-strengthened alloy powders [2–4]. Apart from producing dispersed alloys, Koch et al. [5] also employed the BM technique to prepare amorphous $Ni_{60}Nb_{40}$ alloy, starting from elemental powders of Ni and Nb. This unique process leads to the formation of many advanced materials that cannot be prepared by any other methods, e.g. Al–Nb [6], Al–Ta [7], Ta–Cu [8] and Al–Hf [9] binary systems. Numerous amorphous and metastable (especially those with nanocrystalline microstructures) alloys have been produced by BM and/or rod-milling (RM) techniques [10–37]. The application of the MA process has been expanded recently to produce several metal nitrides [38–42] using a method called reactive ball milling [43].

Whereas all the metal hydrides usually prepared by passing a flow of reactive hydrogen over the metallic materials under high vacuum pressure and at temperatures usually above room temperature (static hydrogenous reaction), in the present study the f.c.c. $NiTiH_3$ solid solution alloy has been synthesized by milling an equiatomic mixture of elemental Ni and Ti powders in a rod mill under a hydrogen gas atmosphere (dynamic hydrogenous reaction). The progress of the hydration reaction including the phase transformation in $NiTiH_3$ alloy powders has been followed by X-ray diffraction (XRD) and transmission electron microscopy (TEM). Moreover, optical microscopy and scanning electron microscopy (SEM) have been used to understand the metallographical and morphological characteristics of the milled alloy powders after several stages of the reactive milling time. The mechanism of the dynamic hydrogenous reaction for the formation of f.c.c. $NiTiH_3$ alloy powders via the RM technique is discussed.

SSDI 0925-8388(94)01367-5

One goal of the present study is to offer an attractive process for the formation of metal hydrides at room temperature by a simple technique.

2. Experimental procedures

High purity (99.9%) elemental Ni (100 μm) and high purity (99.5%) Ti (50 μm) powders, and purified hydrogen and argon gas (H_2O and O_2, less than 10 ppm) have been used. The powders were mixed in a glove-bag under a purified argon atmosphere to give the desired average composition of $Ni_{50}Ti_{50}$. The mixed powders were then charged and sealed in a cylindrical stainless steel shell (SUS 304; 120 mm in diameter) together with stainless steel rods (SUS 304; 10 mm in diameter). The rod-to-powder weight ratio was controlled to be about 30 to 1. The inlet of the shell was connected to a rotary pump and evacuated for about 4 ks. The rod mill was then evacuated for about 7 ks using a diffusion pump. After evacuation, a flow of hydrogen gas was passed carefully into the rod mill through a plastic pipe. Once the rod mill was filled with hydrogen at 1 atm, the inlet of the vial was closed and the reactive rod-milling (RRM) process was carried out at ambient temperature by mounting the rod mill on a rotator at the rate of 1.4 s^{-1}. The RRM was interrupted at selected intervals and a small amount of the rod-milled powder was taken out from the vial in the glove-bag. The alloy powders were characterized by XRD with Cu Kα, SEM operated at 25 kV and TEM using a 200 kV microscope and/or high resolution transmission electron microscopy (HRTEM) operated at 1 MV. The induction-coupled plasma (ICP) emission method was used to analyze the Ni and Ti contents, and the degree of Fe contamination in the milled powder. The oxygen and the hydrogen contents in the alloy powders were detected by the helium carrier fusion–thermal conductivity method. After milling for 720 ks, the iron and oxygen contents in the alloys were determined to be less than 0.60 at.% and 0.90 at.% respectively.

3. Results

3.1. Structural change with the reactive rod-milling time

3.1.1. X-ray diffraction analyses

X-ray analyses were performed in order to understand the total structure of the mechanically alloyed powders milled under the hydrogen gas atmosphere. Fig. 1 displays the XRD patterns of NiTi alloy powders after the starting, first and intermediate stages of the RRM time. At the starting stage of milling (Fig. 1(a)), the initial powders consist of polycrystalline f.c.c. Ni and h.c.p. Ti. After an MA time (first stage) of 11 ks, almost all the Bragg peaks corresponding to h.c.p. Ti had surprisingly disappeared and a new phase of f.c.c. TiH_2 was detected, indicating a solid–gas reaction between the milling atmosphere (hydrogen) and the metallic Ti, as presented in Fig. 1(b). This new phase coexists with unprocessed Ti powders, suggested by the Bragg peaks of Ti(103) and Ti(200). At an intermediate RRM time

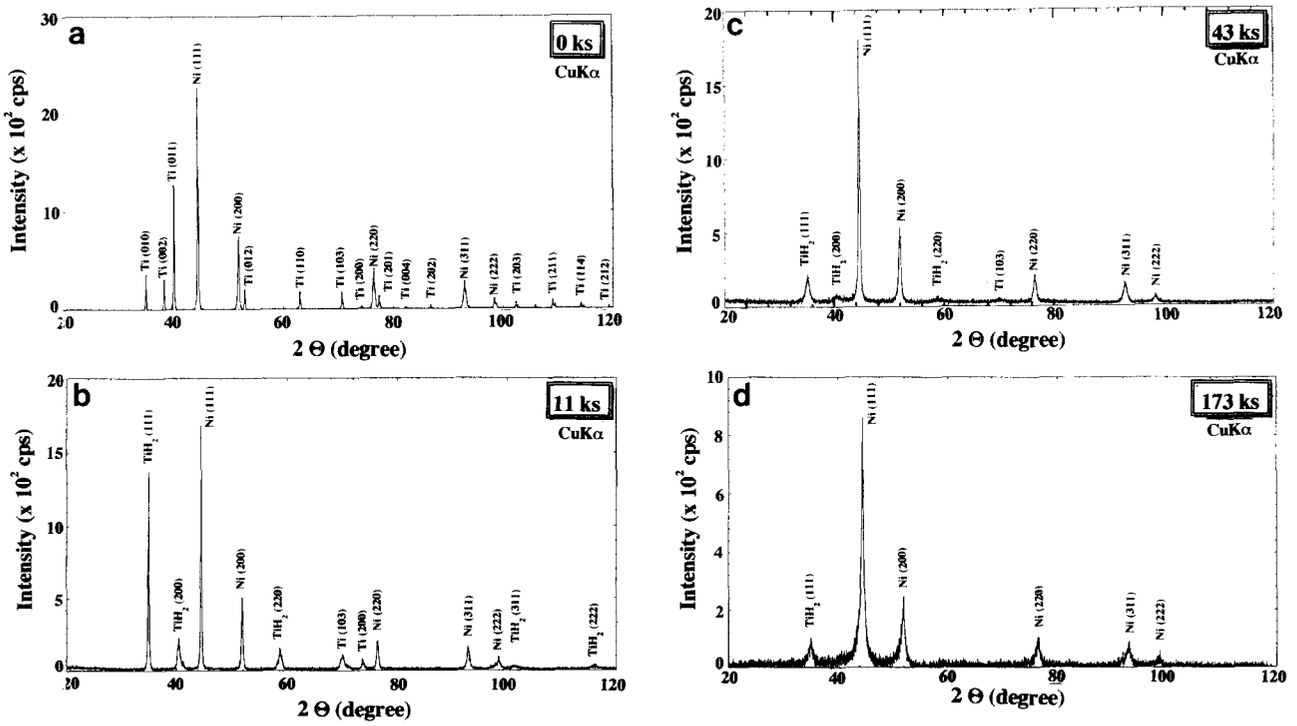

Fig. 1. Typical XRD patterns of $NiTiH_3$ alloy powders at the (a) initial, (b) early and (c), (d) intermediate stages of RRM.

(43 ks), the minor Bragg peaks of h.c.p. Ti had completely disappeared, indicating a complete phase transformation of h.c.p. Ti to f.c.c. TiH_2, as shown in Fig. 1(c). Moreover, the positions of the Bragg peaks for crystalline f.c.c. Ni have shifted markedly to smaller angles, indicating the formation of f.c.c. $NiTiH_3$ solid solution. It is worth noting that after an RRM time of 173 ks, all the major peaks of TiH_2 had disappeared, suggesting a solid state reaction between f.c.c. Ni and f.c.c. TiH_2, as illustrated in Fig. 1(d).

The XRD patterns for the final product of $NiTiH_3$ (360–720 ks), are presented in Fig. 2. Obviously, the Bragg peaks of $NiTiH_3$ become broader and none of the peaks corresponding to TiH_2 are seen. It is worth noting that the broadness of these peaks can be attributed to the formation of fine grains of $NiTiH_3$ solid solution powders, as shown in Fig. 2(a). We should emphasize that this solid solution phase has not changed to any other phase(s), even for samples milled for times as long as 720 ks, as presented in Fig. 2(b). The XRD patterns of the end product (720 ks) of $NiTiH_3$ alloy powders after annealing in a differential scanning calorimeter under a flow of argon at 993 K are presented in Fig. 2(c). Obviously, the Bragg peaks of $NiTiH_3$ have become more pronounced and sharper. Furthermore, the phase of $NiTiH_3$ formed is very stable and has not changed to any other phase, even at this high temperature.

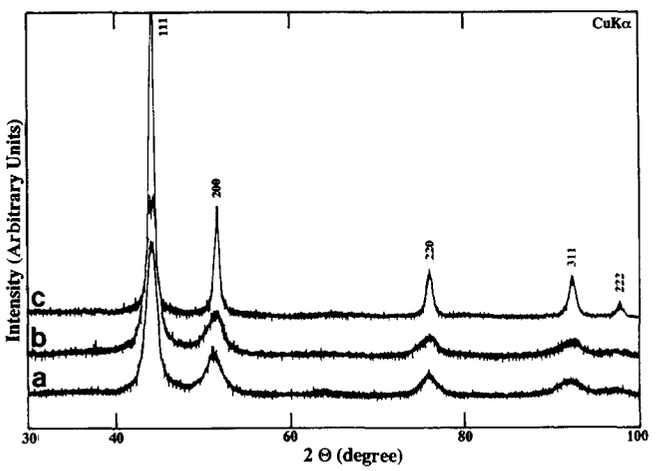

Fig. 2. The XRD patterns of the final products for $NiTiH_3$ alloy powders after RRM for 360 ks (curve a), 720 ks (curve b) and 720 ks (curve c) and then annealing in a differential scanning calorimeter under a flow of argon at 993 K.

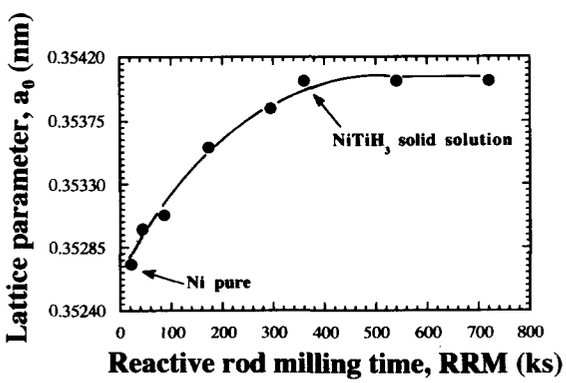

Fig. 3. Effect of the progressive RRM times on the lattice parameter a_0 of $NiTiH_3$ alloy powders.

The lattice parameter a_0 of $NiTiH_3$ estimated from XRD measurements is shown in Fig. 3 as a function of the RRM time. During the first and the intermediate stages of milling, the f.c.c. $NiTiH_3$ solid solution expands with increasing RRM time, characterized by a monotonic increase in a_0. Towards the end of the processing time, the value of a_0 increases to a maximum of 0.35403 nm after 360 ks, as shown in Fig. 3. This value is larger than that of pure f.c.c. Ni (0.3524 nm), suggesting an interstitial solubility of TiH_2 in Ni. No change in a_0 could be obtained even after further milling time (720 ks), indicating the formation of a supersaturated $NiTiH_3$ solid solution.

3.1.2. *Transmission electron microscopy observations*

Detailed TEM analyses were performed in order to understand the change in the local structure of the mechanically alloyed $NiTiH_3$ powder particles during the above-mentioned stages of milling. The bright-field images (BFIs) and/or the dark-field image (DFI), and the selected-area diffraction patterns (SADPs) of $NiTiH_3$ powders after selected RBM times are shown in Fig. 4. Fig. 4(a) shows the BFI and Fig. 4(b) the corresponding SADP of powders at the initial stage (an RRM time of 0 ks). The powders have large grains of about 100 nm diameter and the SADP (Fig. 4(b)) taken at the center of this micrograph shows sharp ring patterns coexisting with spot patterns of pure polycrystalline Ni and Ti crystals. Figs. 4(c)–4(e) show the BFI together with SADPs of the milled powders after an RRM time of 11 ks. The oriented particle has twin and nanotwin boundaries of TiH_2(111) and Ni(111) planes, as shown in the corresponding SADPs of zone I (Fig. 4(d)) and zone II (Fig. 4(e)). Moreover, several defects with grain boundary movement are clearly seen near the center and the edge of the micrographs. Fig. 4(f) shows the HRTEM picture of $NiTiH_3$ alloy powder after an RRM time of 173 ks. The powder particles are homogeneous in structure, and the presented fringe images are related to a single phase of f.c.c. $NiTiH_3$ alloy, as shown in Figs. 4(f) and 4(g). Figure 4(h) shows the DFI and Fig. 4(i) the corresponding SADP of an $NiTiH_3$ powders at the final interval MA processing time. The powder particles have a cell-like morphology containing very fine grains with nanodimensions (about 5 nm or less in diameter). Obviously, the Debye–Scherrer rings of the SADP (Fig. 4(i)) shows the typical structure of the f.c.c. phase, suggesting the formation of $NiTiH_3$ solid solution in good agreement with the XRD patterns in Fig. 2.

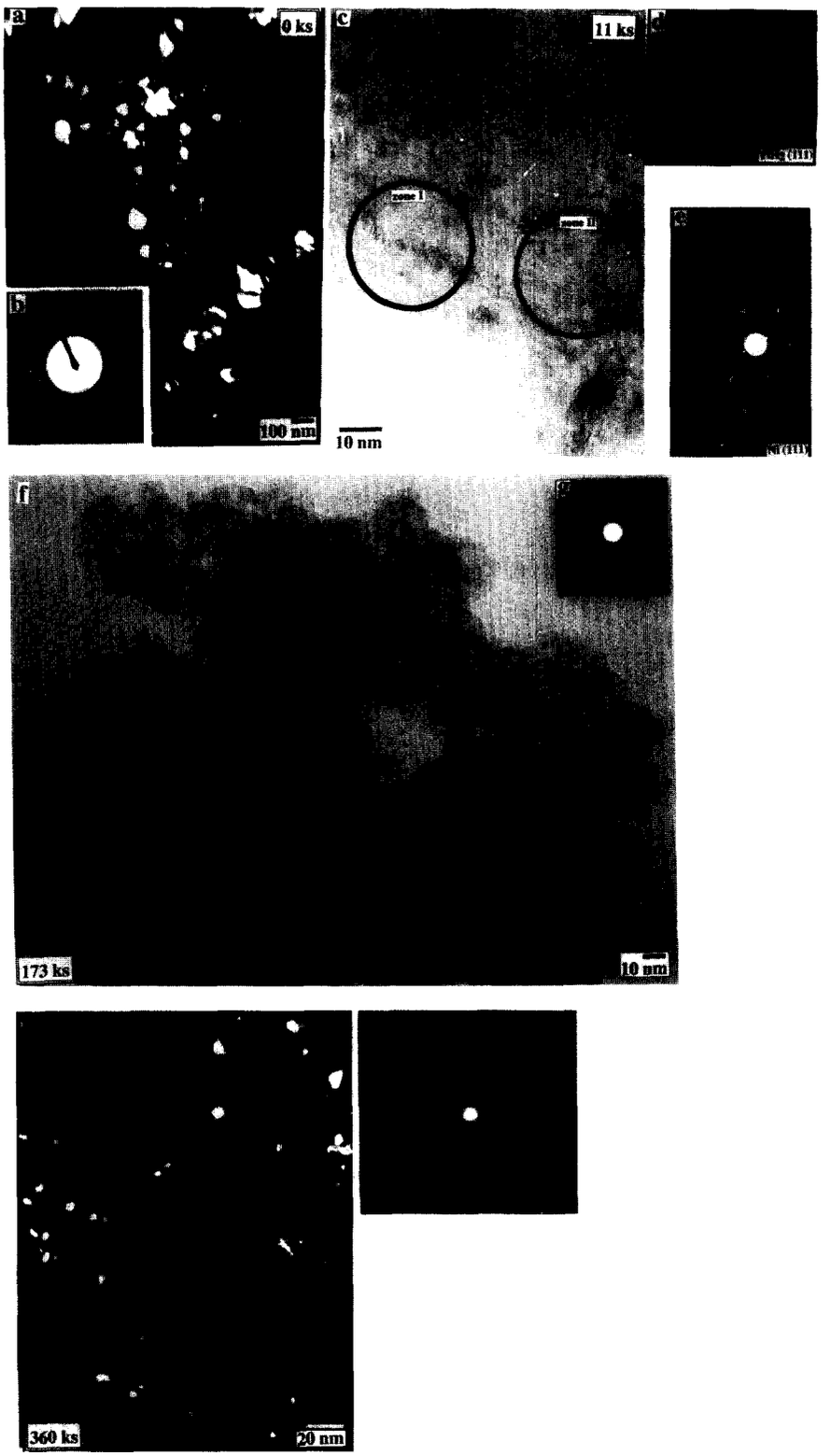

Fig. 4. Detailed TEM observations for $NiTiH_3$ alloy powders after selected RRM times. The BFIs and/or DFI are shown together with SADPs.

3.2. Morphology and metallography changes with the reactive rod-milling time

The SEM technique was used to follow the change in the size and the shape of mechanically alloyed NiTi powder particles milled under a hydrogen gas atmosphere for different RRM times. Detailed SEM observations after several stages of the MA process are presented in Fig. 5. The starting materials of Ni and Ti powders are randomly distributed in size and have

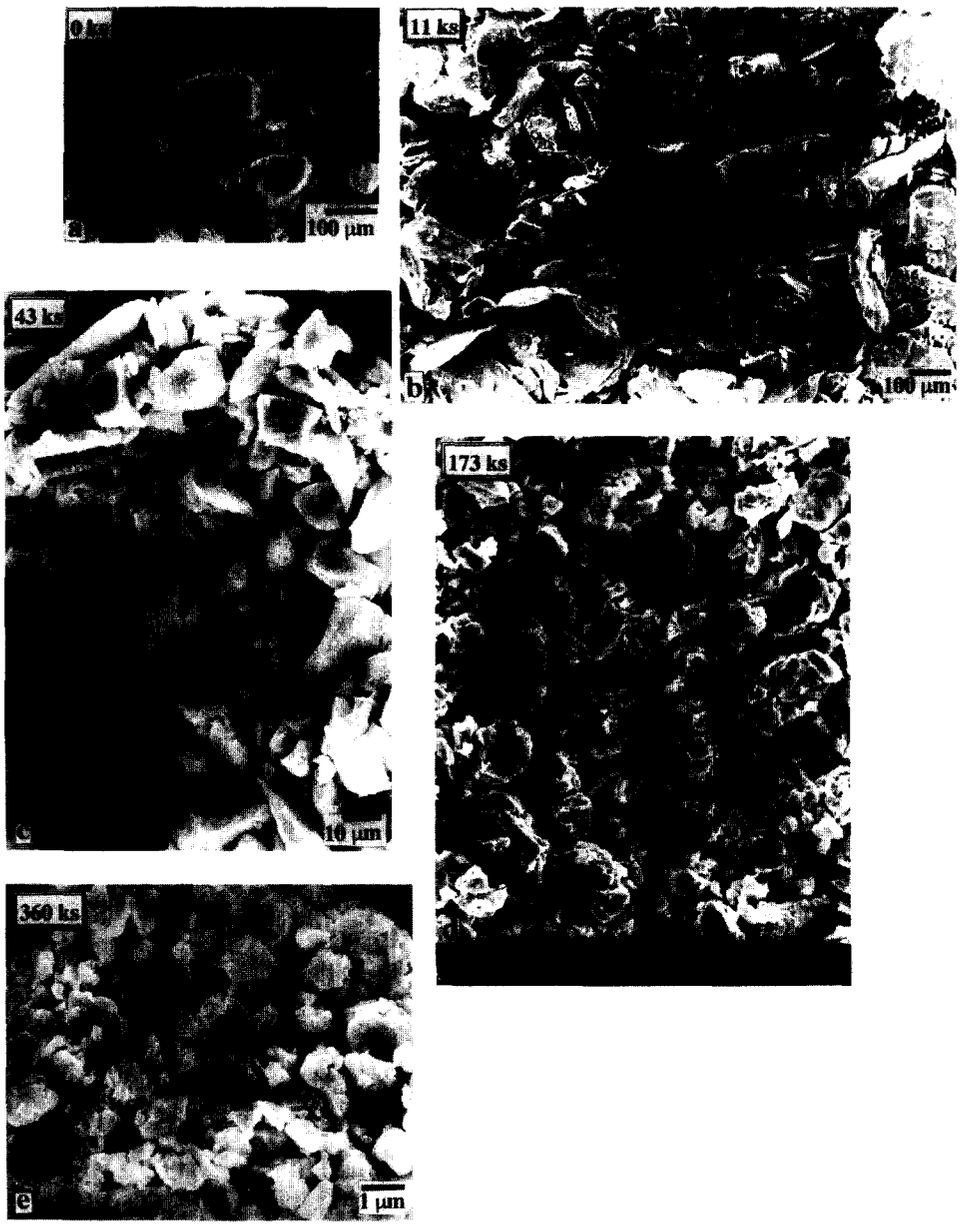

Fig. 5. Scanning electron micrographs of $NiTiH_3$ alloy powders milled for RRM times of (a) 0 ks, (b) 11 ks, (c) 43 ks, (d) 173 ks and (e) 360 ks.

a morphology that is typical for powders of ductile metallic materials, as presented in Fig. 5(a). Fig. 5(b) is a scanning electron micrograph of NiTi after milling in a hydrogen gas atmosphere for 11 ks. Obviously, the powders are a mixture of particles with plate-like (Ni particles) and rod-like morphologies. Contrary to this, those having a rod-like morphology are TiH_2 powders resulting during the solid–gas reaction between hydrogen and Ti powders. The cross-sectional view of the particles of plate-like morphology shows the presence of white micrograins belonging to the TiH_2 phase (brittle grains) in the Ni particle (ductile matrix), as shown in Fig. 6(a). During the progress of the RRM process, the particles have continuously disintegrated to form powder particles that are somewhat irregular in shape (globe- and flake-like morphology) and size (10–40 μm), as shown in Fig. 5(c). The metallographic details near the edge of a composite particle shows an increasing of TiH_2 phase (Fig. 6(b)). As the MA time increases, the size of the powder particles decreases and the particles tend to have a more definite shape with a globe-like morphology, as presented in Fig. 5(d). The optical metallographic examination of the cross-section for polished and etched particles after an RRM time of 173 ks shows that the grain structure morphology has already disappeared, and the individual particles do not have any details on their polished surfaces, as shown in Fig. 6(c). At the end of the MA process (360 ks) the powder particles are fairly uniform in size but vary from 0.5 to 1.5 μm in diameter. Moreover, the

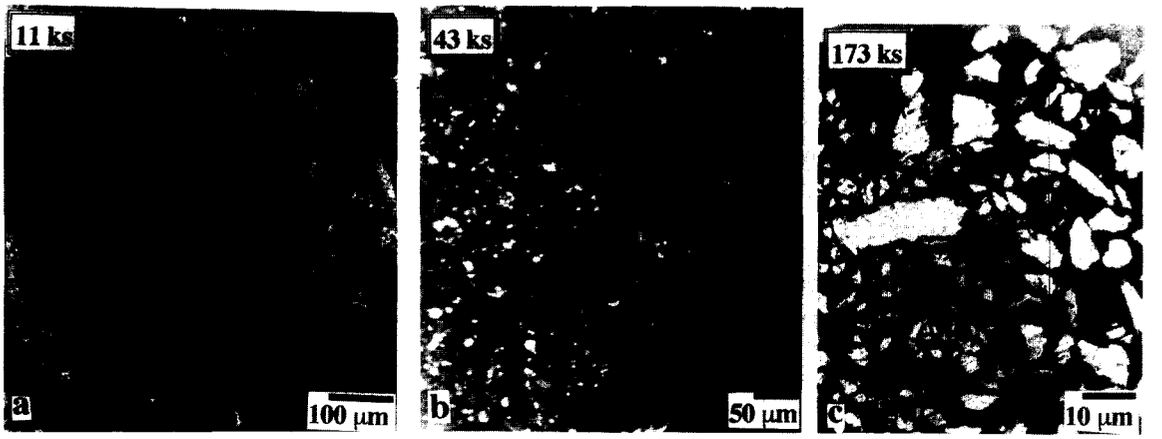

Fig. 6. Optical micrographs for the polished surface of $NiTiH_3$ alloy powders milled for RRM times of (a) 11 ks, (b) 43 ks and (c) 173 ks.

end product of $NiTiH_3$ alloy powders have a smooth spherical-like morphology without any relief details on the surface, as shown in Fig. 5(e).

4. Discussion

As shown by the above experimental results, during the RM of a mixture of equiatomic Ni and Ti elemental powders under a hydrogen gas atmosphere, two types of reaction take place. The first is a typical solid–gas reaction occurring between h.c.p. Ti powders and hydrogen gas. This reaction is followed by a solid state reaction between f.c.c. Ni and the product of the first reaction, i.e. f.c.c. TiH_2 powders. In this section, the role of the formation of $NiTiH_3$ alloy powders via the RM technique is discussed. Fig. 7 may be used to summarize the mechanism of the dynamic solid state hydrogenous reaction.

4.1. The stage of solid–gas reaction

This early stage of RRM (0–11 ks) refers to the reaction between the starting materials of Ni and Ti powders and the milling atmosphere (reactive hydrogen gas). At this stage, the starting elemental powder particles of Ni and Ti (Fig. 7(a)) are subjected to dramatic shear stresses that are generated by the rods as milling media. As a result of this continuous stress, the powder particles disintegrate into smaller particles, and very clean or fresh oxygen-free active surfaces of the powders are created, as illustrated in Fig. 7(b). On the basis of the results of the present study, the reactive hydrogen gas that is initially presented in the rod mill was gettered and absorbed completely by the first atomically clean surfaces of Ti powders to form f.c.c. TiH_2 alloy (Fig. 7(c)) owing to the following forward reaction:

$$Ti(s) + H_2(g) = TiH_2(s) \quad (1)$$

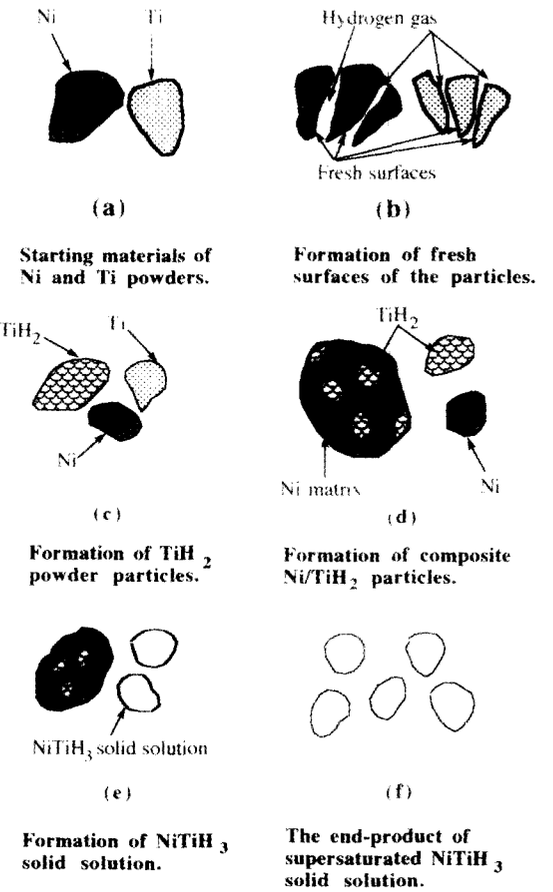

Fig. 7. Proposed flow sheet diagram which illustrates the mechanism of the mechanical solid state hydration reaction via the RRM technique for the $NiTiH_3$ system.

The enthalpy ΔH^{for} of formation for f.c.c. TiH_2 is -38 kJ mol^{-1} [44]. Contrary to this, the ΔH^{for} for Ni_xH_{1-x} has a positive value [44] so that the reaction between Ni and hydrogen cannot occur simultaneously. Thus the end products of this stage are unreacted Ni and TiH_2 powders.

4.2. The stage of solid state reaction

The previous stage of milling is followed by a second stage which is called the stage of solid state reaction (11–360 ks). Since the starting elemental powders of h.c.p. Ti have been transformed completely to the f.c.c. TiH_2 phase, the reaction of the RRM process was changed from a solid–gas reaction (previous stage) to a solid state reaction between the unreacted elemental Ni and TiH_2 powders, as shown in Figs. 4(c) and 7(d). During this second stage of milling, the brittle phase of TiH_2 powder particles penetrates the ductile matrix of Ni to form composite Ni–TiH_2 particles coexisting somewhat with unprocessed Ni and/or TiH_2, as illustrated in Figs. 1(c) and 7(d). As the RRM time increases (173 ks), TiH_2 diffuses simultaneously in the matrix of Ni to form f.c.c. $NiTiH_3$ solid solution, as presented in Figs. 1(d), 4(f), 6(c) and 7(e). We should emphasize that increasing the RRM time leads to a dramatic increase in the value of the lattice parameter a_0 for Ni, indicating the interstitial solubility of TiH_2 in Ni, as was illustrated in Fig. 3. A further increase in RRM time (360 ks) leads to the formation of a supersaturated $NiTiH_3$ solid solution (Fig. 2(a)) which is very stable and does not change to any other phase(s), e.g. amorphous phase, either by further milling or by annealing at a high temperature (993 K), as illustrated in Fig. 2(b) and Fig. 2(c). This can be understood from the fact that the powder particles of $NiTiH_3$ phase are very brittle and decreased sharply during this stage; thus the large amount of strain necessary for amorphous formation cannot be stored.

5. Conclusion

$NiTiH_3$ alloy powder has been fabricated by milling an equiatomic mixture of elemental Ni and Ti powders in a rod mill under reactive hydrogen gas at room temperature. The rod-milled alloy powders have been characterized by means of XRD, optical microscopy, SEM, TEM and chemical analysis. The milling process is classified into two stages in which the end products differ widely from stage to stage. During the first stage, which is called the solid–gas reaction (0–11 ks), coarse powder particles of Ni and Ti disintegrated into several particles that have fresh surfaces. These fresh surfaces are very active and able to absorb hydrogen gas, so that h.c.p. Ti reacts completely with the hydrogen gas to form f.c.c. TiH_2 with grain diameters of about 60 nm. During this hydrogenation process, the Ni powder particles are neutral and do not react with hydrogen (milling atmosphere). At the second stage (11–360 ks) of milling (the stage of solid state reaction) and after milling for 43 ks, the f.c.c. TiH_2 formed diffuses into the Ni matrix to form f.c.c. $NiTiH_3$ solid solution with an average grain diameter of 10 nm. This solid solution expands with increasing rod milling time (173 ks) and becomes saturated to give a constant lattice parameter a_0 of 0.35403 nm after milling for 360 ks. The end product of the f.c.c. $NiTiH_3$ solid solution consists of fine (1 μm in diameter) and homogeneous (spherical-like morphology) powder particles. In addition, the metallic hydride phase formed is very stable at temperatures as high as 993 K.

References

[1] J.S. Benjamin, *Metall. Trans. A, 1* (1970) 2943.
[2] I.G. Wright and A. Wilox, *Metall. Trans. A, 5* (1974) 957.
[3] G.H. Gessinger, *Metall. Trans. A, 1* (1976) 1203.
[4] J.S. Benjamin, *Sci. Am., 40* (1976) 234.
[5] C.C. Koch, O.B. Cavin, C.G. McKamey and J.O. Scarbourgh, *Appl. Phys. Lett., 43* (1983) 1017.
[6] E. Hellstern, L. Schultz, R. Bormann and D. Lee, *Appl. Phys. Lett., 53* (1988) 1399.
[7] M. Sherif El-Eskandarany, F. Itoh, K. Aoki and K. Suzuki, *J. Non-Cryst. Solids, 117–118* (1990) 729.
[8] T. Fukunaga, K. Nakamura, K. Suzuki and U. Mizutani, *J. Non-Cryst. Solids, 117–118* (1990) 700.
[9] M. Sherif El-Eskandarany, K. Aoki, T. Matsumoto and K. Suzuki, *J. Alloys Comp.*, (1994) in press.
[10] C. Politis and W.L. Johnson, *J. Appl. Phys., 60* (1986) 1147.
[11] R. Schwarz and C.C. Koch, *Appl. Phys. Lett., 49* (1986) 146.
[12] P.Y. Lee and C.C. Koch, *J. Non-Cryst. Solids, 94* (1987) 88.
[13] E. Hellstern and L. Schultz, *J. Appl. Phys., 63* (1988) 1408.
[14] K. Suzuki, *J. Non-Cryst. Solids, 112* (1989) 23.
[15] E. Gaffet and M. Harmelin, *J. Less-Common Met., 157* (1990) 201.
[16] M. Sherif El-Eskandarany, K. Aoki and K. Suzuki, *J. Less-Common Met., 167* (1990) 113.
[17] J.S.C. Jang and C. Koch, *J. Mater. Res., 5* (1990) 498.
[18] M. Sherif El-Eskandarany, K. Aoki and K. Suzuki, *Scr. Metall., 25* (1991) 1695.
[19] M. Sherif El-Eskandarany, K. Aoki and K. Suzuki, *J. Alloys Comp., 177* (1991) 229.
[20] M. Sherif El-Eskandarany, K. Aoki and K. Suzuki, *J. Appl. Phys., 72*(7) (1992) 2665.
[21] M. Sherif El-Eskandarany, K. Aoki and K. Suzuki, *Mater. Sci. Forum, 88–90* (1992) 81.
[22] M. Sherif El-Eskandarany, K. Aoki and K. Suzuki, *Metall. Trans. A, 23* (1992) 2131.
[23] M. Sherif El-Eskandarany, K. Aoki and K. Suzuki, *J. Appl. Phys., 71*(6) (1992) 2924.
[24] M. Sherif El-Eskandarany, K. Aoki and K. Suzuki, *J. Alloys Comp., 186* (1992) 15.
[25] M. Sherif El-Eskandarany, K. Aoki and K. Suzuki, *J. Non-Cryst. Solids, 150* (1992) 472.
[26] R.B. Schwarz, S. Srinivasan and P.B. Desch, *Mater. Sci. Forum, 88–90* (1992) 595.
[27] Y. Homma, T. Fukunaga, M. Misawa and K. Suzuki, *Mater. Sci. Forum, 88–90* (1992) 339.
[28] E. Gaffet, F. Faudot and M. Harmelin, *Mater. Sci. Forum, 88–90* (1992) 375.
[29] P. Nash, H. Kim, H. Choo, H. Ardy, S.J. Hwang and A.S. Nash, *Mater. Sci. Forum, 88–90* (1993) 603.
[30] E. Gaffet, N. Malhouroux and M. Abdellaoui, *J. Alloys Comp., 194* (1993) 339.

[31] N. Malhouroux-Gaffet and E. Gaffet, *J. Alloys Comp., 198* (1993) 143.
[32] E. Gaffet and N. Malhouroux-Gaffet, *J. Alloys Comp., 205* (1993) 27.
[33] E. Ma, J. Pagán, G. Cranford and M. Atzmon, *J. Mater. Sci. Res., 8* (1993) 1836.
[34] K.-J. Kim, M. Sherif El-Eskandarany, K. Sumiyama and K. Suzuki, *J. Non-Cryst. Solids, 155* (1993) 165.
[35] D.I. Zhang and T.B. Massalski, *J. Mater. Res., 9* (1994) 53.
[36] E. Ma, *J. Mater. Res., 9* (1994) 592.
[37] M. Sherif El-Eskandarany and H.A. Ahmed, *J. Alloys Comp., 216* (1994) 213.
[38] M. Sherif El-Eskandarany, K. Aoki and K. Suzuki, *Appl. Phys., Lett., 60* (1992) 1562.
[39] M. Sherif El-Eskandarany, K. Sumiyama, K. Aoki and K. Suzuki, *J. Mater. Res., 7* (1992) 888.
[40] K. Aoki, A. Memezawa and T. Matsumoto, *J. Mater. Res., 8* (1993) 307.
[41] M. Sherif El-Eskandarany, *J. Alloys Comp., 203* (1994) 117.
[42] M. Sherif El-Eskandarany, K. Sumiyama, K. Aoki, T. Masumoto and K. Suzuki, *J. Mater. Res.*, (1994) in press.
[43] M. Sherif El-Eskandarany, K. Sumiyama, K. Aoki and K. Suzuki, *Mater. Sci. Forum, 88–90* (1992) 801.
[44] F.R. de Boer, R. Boom, W.C.M. Mattens, A.R. Miedema and A.K. Niessen, *Cohesion in Metals–Transition Metal Alloys*, North-Holland, Amsterdam, 1988.